

S.F. Klovanič, Prof., DrSc.
Faculty of Technical Sciences, University of Warmia and Mazury in Olsztyn, Poland
L. Małyżko
Department of Mechanics and Fundamentals of Building Design, Poland

SOIL PLASTICITY IN FINITE ELEMENTS

The phenomenological model for a soil in the form of the associated theory of the plasticity, based on a loading surface of the closed form, is formulated. The analytical form of this surface is offered. Dilatancy, deformation hardening and softening are considered. The paper is focused on nonlinear analysis using finite elements method. The examples of calculations, confirming reliability of model, are proposed.

Keywords: constitutive model of soil, plasticity, finite elements method.

С.Ф. Клованич, д.т.н., професор
Факультет технічних наук, Вармінсько-Мазурський університет в Ольштині, Польща
Л. Малижко
Відділ механіки і фундаментів проектування будівель, Польща

ПЛАСТИЧНА МОДЕЛЬ ҐРУНТУ В СКІНЧЕННИХ ЕЛЕМЕНТАХ

Сформульовано феноменологічну модель ґрунту у формі асоційованої теорії пластичності, що базується на поверхні завантаження замкнутої форми. Наведено аналітичну форму цієї поверхні. Розглянуто процеси дилатанції, деформаційного зміцнення та ослаблення. Виконано нелінійний аналіз з використанням методу скінченних елементів. Наведено приклади розрахунків, що підтверджують достовірність моделі.

Ключові слова: основна модель ґрунту, пластичність, метод скінченних елементів.

С.Ф. Клованич, д.т.н., профессор
Факультет технических наук, Варминско-Мазурский университет в Ольштыне, Польша
Л. Малыжко
Отделение механики и фундаментов проектирования зданий, Польша

ПЛАСТИЧЕСКАЯ МОДЕЛЬ ГРУНТА В КОНЕЧНЫХ ЭЛЕМЕНТАХ

Сформулирована феноменологическая модель грунта в форме ассоциированной теории пластичности, которая основана на поверхности загрузки замкнутой формы. Приведена аналитическая форма этой поверхности. Рассмотрены процессы дилатации, деформационного упрочнения и разупрочнения. Выполнено нелинейный анализ с использованием метода конечных элементов. Приведены примеры расчетов, которые подтверждают достоверность модели.

Ключевые слова: основная модель грунта, пластичность, метод конечных элементов.

Introduction. The theory of a plastic flow with hardening is formulated in the form of relations between increments of deformations $d\{\varepsilon\}$ and stresses $d\{\sigma\}$ and defined as [1]

$$d(\sigma) = [D]_{ep} d\{\varepsilon\}, \quad (1)$$

where $[D]_{ep}$ – elastic-plastic stiffness matrix

$$[D]_{ep} = [D] - \frac{[D] \frac{\partial Q}{\partial \{\sigma\}} \left(\frac{\partial F}{\partial \{\sigma\}} \right)^T [D]}{\left(\frac{\partial F}{\partial \{\sigma\}} \right)^T [D] \frac{\partial Q}{\partial \{\sigma\}} + \Lambda}, \quad (2)$$

where $[D]$ – initial elastic matrix, corresponding to the Hook's law for an isotropic material; F and Q – loading function and plastic potential (for associated theory $Q=F$); Λ – hardening function. If a hardening measure χ is the work of stresses on the plastic deformations $\{\varepsilon_p\}$, and $d\chi = \{\sigma\}^T d\{\varepsilon_p\}$, that hardening function is defined so

$$\Lambda = - \frac{\partial F}{\partial \chi} \{\sigma\}^T \frac{\partial F}{\partial \{\sigma\}} = - \frac{\partial F}{\partial \{\varepsilon_p\}} \frac{\partial F}{\partial \{\sigma\}}. \quad (3)$$

The plastic strain rate is normal to the surface, represented by loading function F . This surface usually build in local cylindrical octahedral coordinates σ_o, τ_o, θ , where

$$\begin{aligned} \sigma_o &= \frac{1}{3}(\sigma_x + \sigma_y + \sigma_z); \quad \tau_o = \sqrt{\frac{2}{3}} \sqrt{J_2}; \\ \theta &= \frac{1}{3} \arccos \left(\sqrt{2} \frac{J_3}{\tau_o^3} \right). \end{aligned} \quad (4)$$

Here J_2 and J_3 – the second and third stresses invariants.

$$J_2 = -s_x s_y - s_y s_z - s_x s_z + \tau_{xy}^2 + \tau_{yz}^2 + \tau_{xz}^2;$$

$$s_x = \sigma_x - \sigma_o; \quad s_y = \sigma_y - \sigma_o; \quad s_z = \sigma_z - \sigma_o;$$

$$J_3 = s_x s_y s_z - s_x \tau_{yz}^2 - s_y \tau_{xz}^2 - s_z \tau_{xy}^2 - 2\tau_{xy} \tau_{yz} \tau_{xz}.$$

In these coordinates $\{\sigma\} = \{\sigma_o \ \tau_o\}$ и $\{\varepsilon\} = \{\varepsilon_o \ \gamma_o\}$, where

$$\varepsilon_o = \frac{1}{3}(\varepsilon_x + \varepsilon_y + \varepsilon_z); \quad \gamma_o = 2\sqrt{\frac{2}{3}} \sqrt{J_{2\varepsilon}};$$

$$J_{2\varepsilon} = -e_x e_y - e_y e_z - e_x e_z + \frac{1}{4}(\gamma_{xy}^2 + \gamma_{yz}^2 + \gamma_{xz}^2);$$

$$e_x = \varepsilon_x - \varepsilon_o; \quad e_y = \varepsilon_y - \varepsilon_o; \quad e_z = \varepsilon_z - \varepsilon_o,$$

where ε_o and γ_o – octahedral longitudinal and shear deformations; $J_{2\varepsilon}$ – second invariant of a deviator of deformations. The initial matrix of elasticity $[D]$ in this case will look like

$$[D] = \begin{bmatrix} 3K_o & 0 \\ 0 & G_o \end{bmatrix}, \quad (5)$$

where K_o and G_o – the volumetric and shear modulus. Having carried out matrix multiplication and addition, expression (2) can be presented in a usual form

$$[D]_{ep} = \begin{bmatrix} 3K & 0 \\ 0 & G \end{bmatrix}, \quad (6)$$

Where

$$3K = 3K_o - \lambda(a_{11} + a_{12}d\varepsilon_o / d\gamma_o) / \Delta;$$

$$G = G_o - \lambda(a_{22} + a_{12}d\gamma_o / d\varepsilon_o) / \Delta.$$

Here

$$a_{11} = 9K_o^2(\partial F / \partial \sigma_o)^2; \quad a_{12} = 3K_o G_o(\partial F / \partial \sigma_o)(\partial F / \partial \tau_o);$$

$$a_{22} = G_o^2(\partial F / \partial \tau_o)^2; \quad \Delta = -(a_{11} + a_{12}) / (3K_o) - \\ - \partial F / \partial \chi [\sigma_o(\partial F / \partial \sigma_o) + \tau_o(\partial F / \partial \tau_o)].$$

Loading function. Expression for a loading surface is accepted as follows

$$F(\sigma_o, \tau_o, \theta) = \tau_o - A_o(b + \sigma_o)\sqrt{a - \sigma_o} = 0. \quad (7)$$

This surface always passes through a point of current loading σ_o, τ_o , closed from two sides and crosses an axis σ_o in points $-b$ and a (fig. 1). In addition on function (7) following conditions are imposed

$$\tau_o|_{\sigma_o=0} = c_o; \quad \partial \tau_o / \partial \sigma_o|_{\sigma_o=0} = M_o, \quad (8)$$

which allow to establish following relations between parameters of a equation (7)

$$A_o = \frac{2\sqrt{a}}{2a+b} M_o; \quad b = \frac{2ac_o}{2aM_o - c_o}. \quad (9)$$

The parameter a also can be established from (7). It can be defined also approximately

$$a \approx \frac{\sigma_o}{1 - \left(\frac{\tau_o}{M\sigma_o}\right)^2} + b. \quad (10)$$

The curve (4) asymptotic comes nearer to a limiting failure line on Mohr $\tau_o = M_o\sigma_o + c_o$ (Fig.1). Thus the site under a this line corresponds to a hardening zone, above line – softening zone. On the stresses-strains diagram $\tau_o - \gamma_o$ (Fig. 1b) it conforms to an ascending and descending branches. Besides, the derivative of function (4) changes a sign on a site from $-b$ to a . Change of a sign of a derivative is the transfer from contraction to dilatancy. General view of loading surface and its characteristic sections are presented on fig. 2. So-called, deviational section of this surface is a curvilinear triangle with maximal τ_1 and minimal τ_2 radiuses (fig. 2), corresponding to extreme values of a corner $\theta = \pi/3$ at $\sigma_1 = \sigma_2 > \sigma_3$ and $\theta = 0$ at $\sigma_1 > \sigma_2 = \sigma_3$. Thus on the Coulomb

$$\begin{aligned}
 M_1 &= 2\sqrt{2} \frac{\sin \varphi}{3 - \sin \varphi}; & M_2 &= 2\sqrt{2} \frac{\sin \varphi}{3 + \sin \varphi}; \\
 c_1 &= 2\sqrt{2} \frac{\cos \varphi}{3 - \sin \varphi} c; & c_2 &= 2\sqrt{2} \frac{\cos \varphi}{3 + \sin \varphi} c,
 \end{aligned}
 \tag{11}$$

where φ and c – corner of an internal friction and coupling.

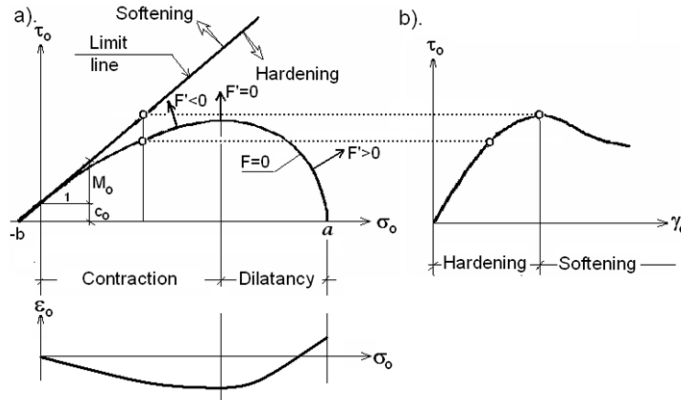


Fig. 1. a – Loading function; b – diagram $\tau_0 - \gamma_0$

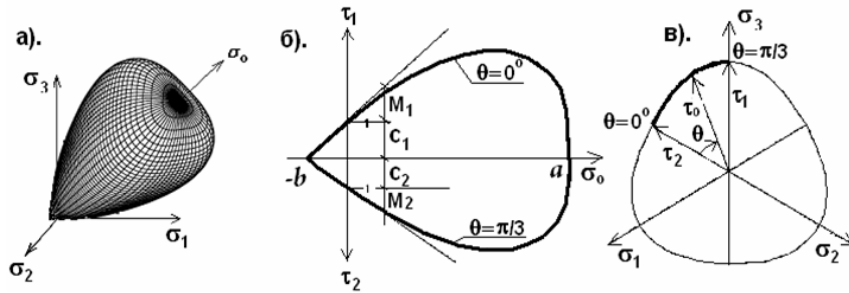


Fig. 2. General view of a surface and its intersections

Between two limiting cases $\theta=0$ and $\theta=\pi/3$ it is possible to present interpolation so [4]

$$\rho(\theta) = 1 - 4(1 - g) \cos \beta (1 - \cos \beta), \quad \beta = \frac{\pi}{3} - \theta, \tag{12}$$

where $g = \frac{3 - \sin \varphi}{3 + \sin \varphi}$. Thus $\rho(0) = 1$ and $\rho(\pi/3) = g$. Then parameters of the formula (7) can be defined so $M_o = \rho(\theta)M_1$, $c_o = \rho(\theta)c_1$, and

$$A_o = \rho(\theta)A_1; \quad A_1 = \frac{2\sqrt{a}}{2a + b} M_1. \tag{13}$$

Hardening and softening. Change of porosity at process of loadings and unloadings is taken as additional measures of hardening. Thus volume porosity of a ground is defined depending on octahedral normal pressure [3, 5] $e = e^o - \mu \ln \sigma_o$ – at active loading; $e = e^A - \delta \ln \sigma_o$ – at unloading, where e^o – porosity in natural state; e^A – porosity of a ground by the time of unloading; μ

and δ – the experimental parameters. The volumetric strains, caused by change of porosity, are defined so

$$3\varepsilon_o = -\frac{e - e_o}{1 + e}, \quad 3d\varepsilon_o = -\frac{de}{1 + e}. \quad (14)$$

Increment of a plastic part of the volumetric strains connected with change of porosity, are equal $d\varepsilon_o^p = d\varepsilon_o - d\varepsilon_o^e$, where $d\varepsilon_o^e$ – elastic strains,

$$3d\varepsilon_o^p = \frac{\mu - \delta}{(1 + e)\sigma_o} d\sigma_o. \quad (15)$$

From (15) it is possible to receive expression for a derivative, entering into a equation (3).

$$\frac{\partial F}{\partial \chi} = \frac{3(1 + e)}{\mu - \delta} \frac{\partial F}{\partial \sigma_o}. \quad (16)$$

At softening the derivative $\frac{\partial F}{\partial \chi}$ is defined from the stresses-strains diagrams (fig. 1, b)

$$\frac{\partial F}{\partial \chi} = \frac{1}{\tau_o} \frac{\partial F}{\partial \tau_o} \frac{\partial \tau_o}{\partial \gamma_o}.$$

Let's notice, that unloading is carried out under the nonlinear, logarithmic law with modules $K_o = \frac{1 + e}{\delta} \sigma_o$; $G_o = \frac{3K_o(1 - 2\nu)}{2(1 + \nu)}$, where ν – coefficient of cross deformations. Thus, as usual at the unloading, the second composed in (2) is equal to zero.

If stresses lies above a limit straight line (fig. 1a), i.e. is in a softening zone, ratios lose meaning since Drukker's known postulate is thus broken. Nevertheless this effect in real experiences is observed, process of deformation is carried out on a falling branch of the diagram (fig. 1b). Therefore that to consider it, expression (16) it is representate in a look

$$\frac{\partial F}{\partial \chi} = \frac{1}{\tau_o} \frac{\partial F}{\partial \tau_o} \frac{\partial \tau_o}{\partial \gamma_o^p} = \frac{1}{\tau_o} G_p \frac{\partial F}{\partial \tau_o} = \frac{1}{\tau_o} \frac{G_o G}{G_o - G} \frac{\partial F}{\partial \tau_o}, \quad (17)$$

where G_p – the plastic shear modulus. The tangent plastic shear modulus we will define, having set analytical expression for a curve in fig. 1b, for example, in a form

$$\xi = \frac{k\eta}{1 + (k - 2)\eta + \eta^2}, \quad (18)$$

where $\xi = \frac{\tau_o}{\hat{\tau}_o}$; $\eta = \frac{\gamma_o}{\hat{\gamma}_o}$; $k = G_o \frac{\hat{\gamma}_o}{\hat{\tau}_o}$.

Here $\hat{\gamma}_o$ and $\hat{\tau}_o$ – top coordinates of the diagram. If differentiate (18) on γ_o , we will receive

$$G = \frac{\partial \tau_o}{\partial \gamma_o} = G_o \left[\frac{1 - \eta^2}{1 + (k - 2)\eta + \eta^2} \right]. \quad (19)$$

Model testing and examples. The model is included in computer program «Concord» [2], realizing a finite elements method. Let's result a test problem about action of a square rigid stamp on a ground and we will compare results of calculations with experimental data [5]. The sizes of a stamp are 40x40 sm. Steps of loading are 40 кН/м². For calculation volume isoparametrical eight-nodes finite elements were used. The symmetric part of the sample was considered only. Ground characteristics: E=2.5 МПа, φ=18°, c=0.045 МПа, ν=0.35. Results of calculation of vertical displacements of a stamp are presented on fig. 3. Here isolines of displacements (fig. 3, a) and stresses (fig. 3, b, c) are given at q=680 кН/м².

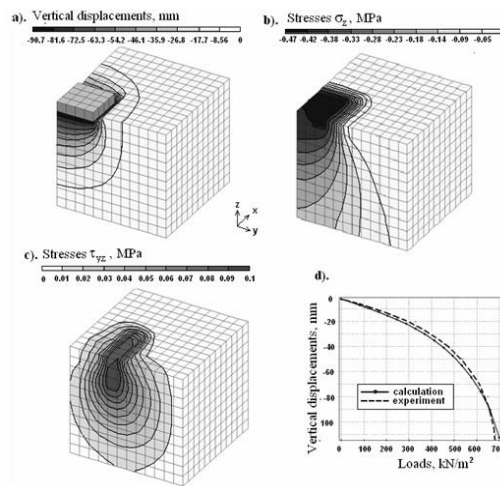


Fig. 3. Results of test

Example 1. Laboratory Studied Sheet Piling Wall. Behavior of the model of steel sheet piling wall was studied in laboratory conditions [6]. Also it was calculated according to presented method. The scheme and layout of the wall as well as soil parameters are presented on fig. 4. 2-D plane strain state is considered. Some results of calculations (continuous lines) and experimental data (dotted lines) are presented on fig. 5 – 8.

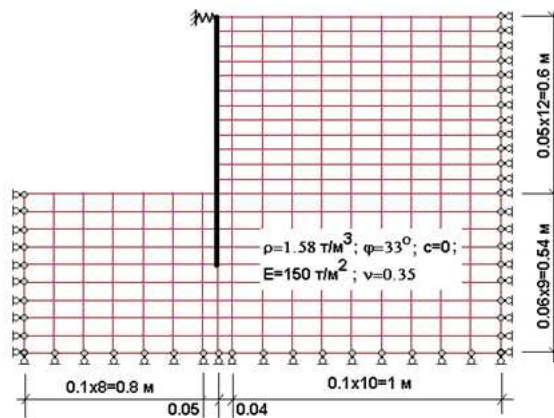


Fig. 4. Laboratory steel sheet piling wall

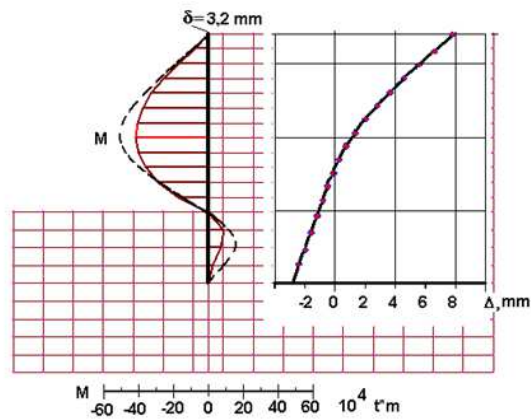


Fig. 5. The moment and active pressure in a wall with thickness 3.2 mm from weight of a soil

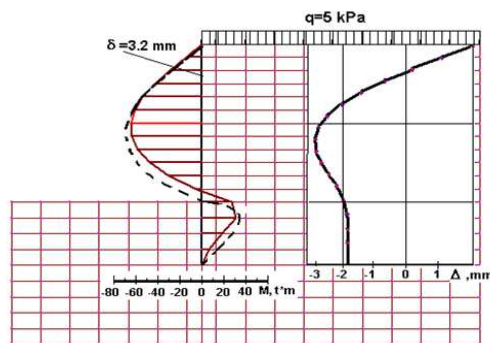


Fig. 6. The moment and active pressure in a wall 3.2 mm from the distributed loading

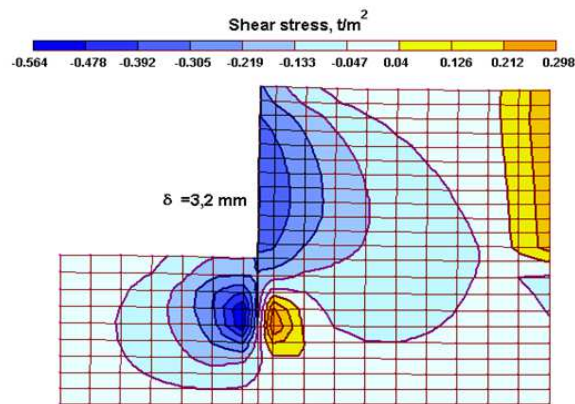


Fig. 7. The shear stresses in a wall 3.2 mm from the distributed loading

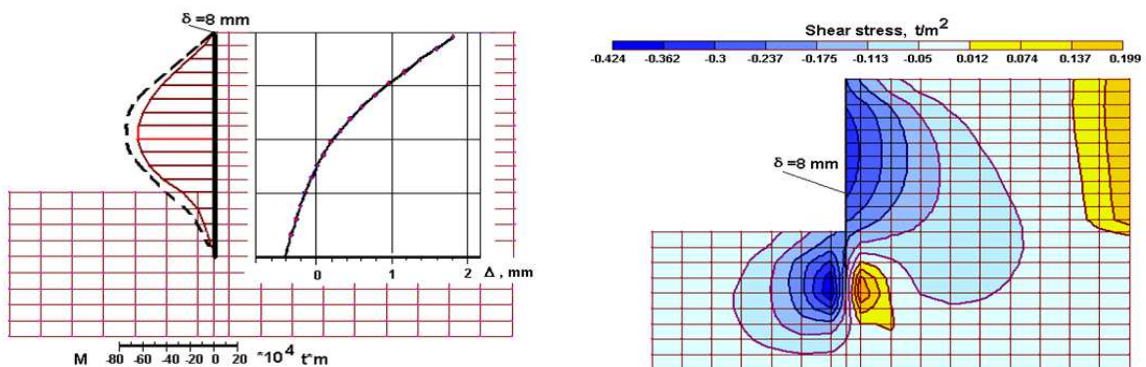


Fig. 8. The moment, active pressure and shear stresses in a wall 8 mm from weight of soil

Example 2. Reinforced Concrete Anchored Sheet Piling Wall. Behavior of reinforced concrete anchored sheet piling wall was studied in Donetsk port (Ukraine) according to the work [7]. Some results of calculations (continuous lines) and measured on site values (dotted lines) are presented on fig. 9 – 10.

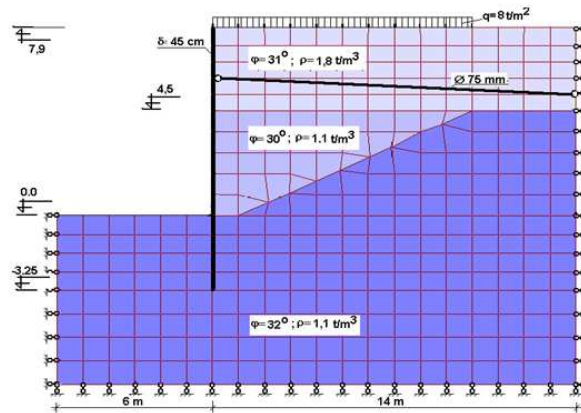


Fig. 9. Reinforced concrete anchored sheet piling wall

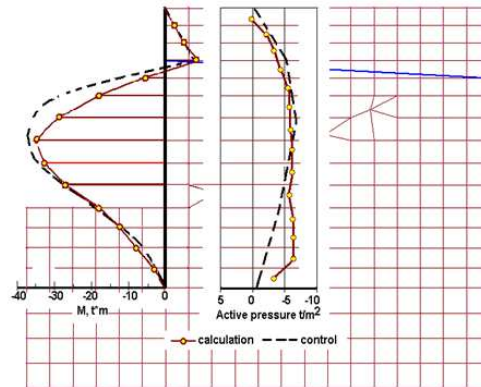


Fig. 10. Moment and active pressure in anchored sheet piling wall

Example 3. Limiting condition of a slope. Let's put an example of calculation stress-strain state and limiting condition of a slope, on border which one the stamp acts. The computational scheme is show on a fig. 11. The plane elements by depth 100 cm will be used. The characteristics of a soil: modulus $E=5000$ MPa, Poisson's ratio $\nu=0.35$, weight $\rho=1.8$ t/m³, angle of internal friction $\phi=30^\circ$, coupling $c=5$ MPa.

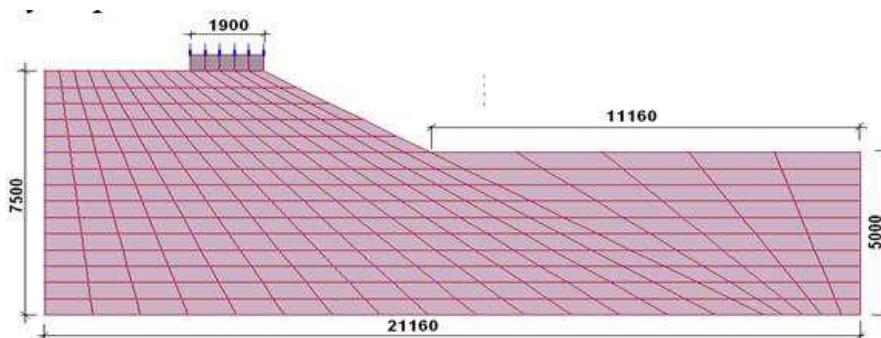


Fig. 11. Slope

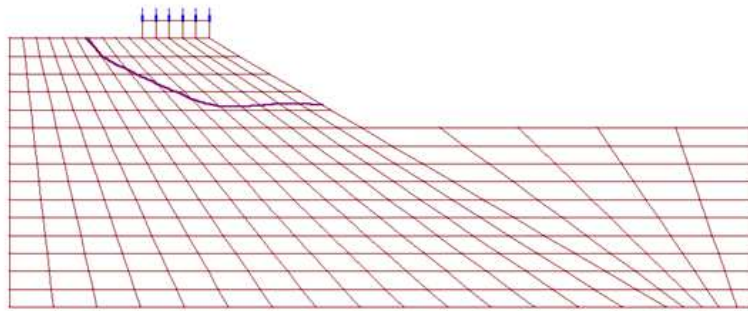


Fig. 12. Areas of a unstable state

The load to stamp was applied sequentially by stages on 50 kN. The process of loading was automatically intercepted at the moment of achievement of a limiting unstable of a slope, comes of calculations are shown in a fig. 12–14. In a fig. 12 the areas of a unstable state of a soil are submitted. The limit's area is a slip line. The strained state of a slope at the moment of loss of stability is rotined in a fig. 13. The vertical displacement of a stamp are shown in a fig. 14.

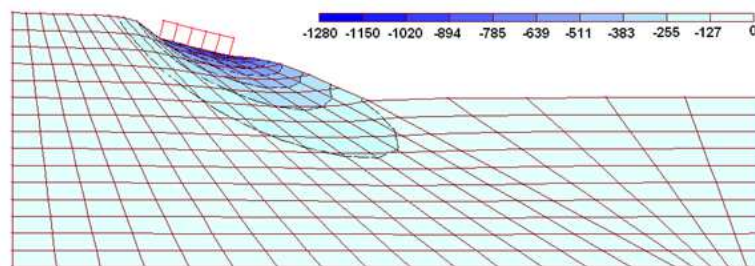


Fig. 13. Vertical displacement

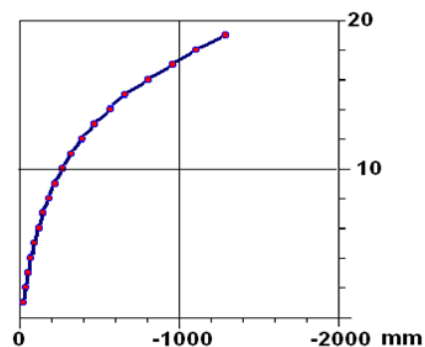


Fig. 14. Vertical displacement of a stamp

Example 4. Ground bank. And in summary we shall demonstrate an example of calculation of a ground bank under only weight. The bank is erected layerwise from a soil with the following characteristics: modulus $E=3000$ MPa, Poisson's ratio $\nu=0.35$, volume weight $\rho=2.0$ t/m³, angle of internal friction $\varphi=18^\circ$, coupling $c=10$ MPa. The computational scheme of a bank is adduced in a fig. 15. The process of level-by-level escalating is modelled step-by-step change of the computational scheme during step calculation. At each stage of calculation the horizontal layer of elements is added. The external loading, except weights of a soil, misses. In a fig. 16–18 the izolines of vertical displacement on some

stages of loading are added. In a fig. 17–19 the shearing stresses of calculation are rotated.

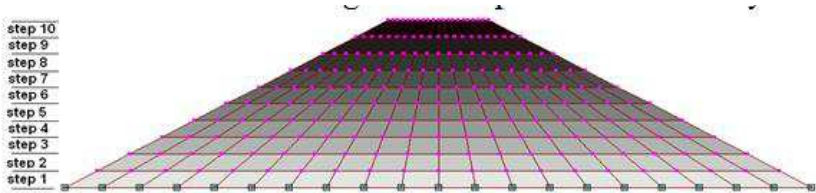


Fig. 15. Computational scheme of a bank

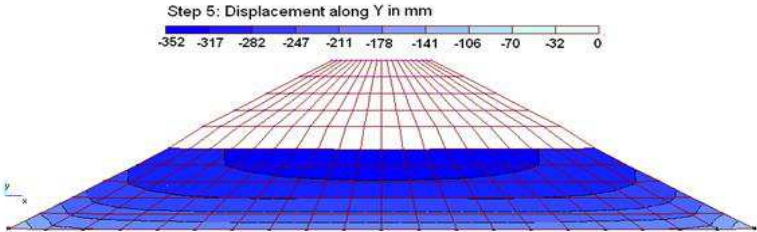


Fig. 16. Vertical displacements at 5 step

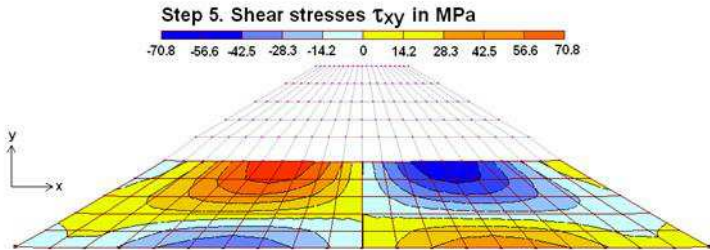


Fig. 17. Shear stresses at 5 step

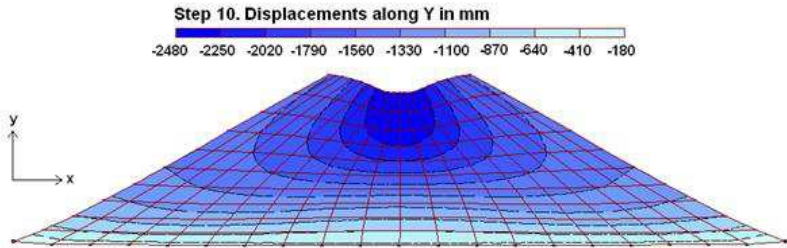


Fig. 18. Vertical displacements at 10 step

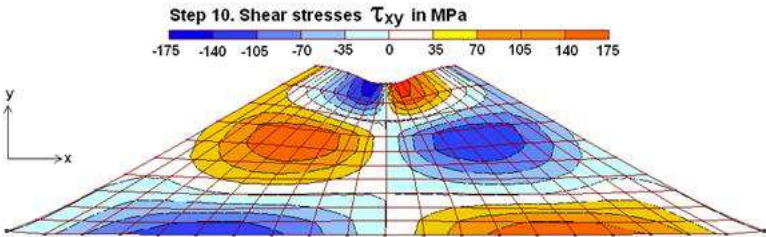


Fig. 19. Shear stresses at 10 step

Conclusion. Comparison of known experimental data with calculated values of main parameters of structure soil stresses-deformed state (some examples of such analysis were presented above) demonstrated effectiveness of proposed model and method of its realization.

Literatures

1. Zienkiewicz O.C. *The Finite Element Method* / O.C.Zienkiewicz, R.L.Taylor. – Oxford: Butterworth-Heinmann, *Solid Mechanics, fifth ed.*, 2000. – Vol. 2. – 220 p.
2. Klovanich S.F. *Finite elements method in nonlinear problems of engineering mechanics* / S.F. Klovanich. – Zaporozhie, 2009. – 400 p.
3. Terzaghi K. *Soil Mechanics in Engineering Practice* / K.Terzaghi, Ralph B. – New York: John Wiley and Sons, 1967. – 350 p.
4. Roscoe K.J. *Mechanical Behavior of an Idealised “Wet” Clay* / K.J Roscoe, A.N.Schofield // *Proc. 1st European Conf. on Soil Mechanics and Foundation Engineering.* – 1963. – P. 47–54.
5. Balura M.V. *Horizontal displacements of the basis under a rigid stamp* / M.V. Balura // *Osnovania, fundamenti i mehanika gruntov.*–1973. – №6. – P. 39–41.
6. Pereviazkin Y.A. *Laboratory study of anchored sheet pilings* / Y.A.Pereviazkin // *Scientific Papers.* – Leningrad, 1987. – 75 p.
7. Gurevich V.B. *River port hydrotechnical structures* / V.B. Gurevich. – Moscow: “Transport”, 1969. – 550 p.

Надійшла до редакції 23.09.2013

© С.Ф. Клованич, Л. Малижко